

 Open access • Journal Article • DOI:10.1038/NMAT2479

Rational design and application of responsive α -helical peptide hydrogels

— [Source link](#) 

Eleanor F. Banwell, ES Abelardo, ES Abelardo, Dave J. Adams ...+7 more authors



Institutions: University of Bristol, Bristol Royal Infirmary, University of Liverpool, University of Sussex

Published on: 01 Jul 2009 - Nature Materials (Nature Publishing Group)

Topics: Self-healing hydrogels, Rational design and Tissue engineering

Related papers:

- [Self-assembly and mineralization of peptide-amphiphile nanofibers](#)
- [Controlling hydrogelation kinetics by peptide design for three-dimensional encapsulation and injectable delivery of cells](#)
- [Responsive Hydrogels from the Intramolecular Folding and Self-Assembly of a Designed Peptide](#)
- [Selective Differentiation of Neural Progenitor Cells by High-Epitope Density Nanofibers](#)
- [Spontaneous assembly of a self-complementary oligopeptide to form a stable macroscopic membrane.](#)

Share this paper:    

View more about this paper here: <https://typeset.io/papers/rational-design-and-application-of-responsive-a-helical-16o4qb8a4a>

Rational design and application of responsive α -helical peptide hydrogels

Eleanor F. Banwell¹, Edgardo S. Abelardo^{1,2}, Dave J. Adams^{3*}, Martin A. Birchall², Adam Corrigan⁴, Athene M. Donald⁴, Mark Kirkland³, Louise C. Serpell⁵, Michael F. Butler^{3†} and Derek N. Woolfson^{1,6†}

Biocompatible hydrogels have a wide variety of potential applications in biotechnology and medicine, such as the controlled delivery and release of cells, cosmetics and drugs, and as supports for cell growth and tissue engineering¹. Rational peptide design and engineering are emerging as promising new routes to such functional biomaterials^{2–4}. Here, we present the first examples of rationally designed and fully characterized self-assembling hydrogels based on standard linear peptides with purely α -helical structures, which we call hydrogelating self-assembling fibres (hSAFs). These form spanning networks of α -helical fibrils that interact to give self-supporting physical hydrogels of >99% water content. The peptide sequences can be engineered to alter the underlying mechanism of gelation and, consequently, the hydrogel properties. Interestingly, for example, those with hydrogen-bonded networks of fibrils melt on heating, whereas those formed through hydrophobic fibril–fibril interactions strengthen when warmed. The hSAFs are dual-peptide systems that gel only on mixing, which gives tight control over assembly⁵. These properties raise possibilities for using the hSAFs as substrates in cell culture. We have tested this in comparison with the widely used Matrigel substrate, and demonstrate that, like Matrigel, hSAFs support both growth and differentiation of rat adrenal pheochromocytoma cells for sustained periods in culture.

As our understanding of sequence-to-structure relationships in proteins improves, so does our ability to rationally design new proteins and protein-based materials. Unlike discrete peptide and protein objects, the design of biomaterials requires extra rules for self-assembly to enable the nano-to-micrometre scale regimes to be bridged^{2,4}. In these respects, synthetically accessible peptides—which can be programmed to fold into prescribed structures, and to self-assemble into larger architectures—offer routes to rationally designed peptide and protein-based biomaterials. Indeed, a variety of peptide-based self-assembling fibres, tapes and hydrogels have been produced^{6–11}. Much of this effort has been directed to the assembly of β -structured systems, although α -helix-based fibrous and α -helix-containing gelling materials have been explored to some extent^{8,12–17}.

Previously, we have described a number of fibrous biomaterials based on the α -helical coiled coil^{8,18,19}. These so-called SAFs (self-assembling fibres) comprise two 28-residue peptides designed to co-assemble, resulting in an offset α -helical dimer with complementary sticky ends. The ends promote longitudinal assembly into α -helical

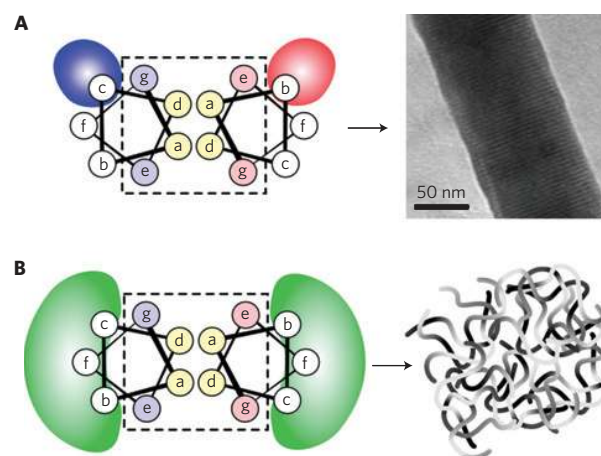


Figure 1 | hSAF design principles. **A**, In previous SAF designs, specific charged interactions between certain b and c positions lead to peptide alignment and fibre thickening. **B**, For the hSAFs, we replaced these specific interactions with weaker, more-general interactions at all b, c and f sites, to result in smaller, more flexible, bundles of thinner fibres.

coiled-coil fibrils, which bundle to form matured fibres. Elsewhere, we have demonstrated that specific interactions—fostered by features on the surface of the coiled coil—lead to crystallization of the peptides within the fibres, Fig. 1a (ref. 19). Consequently, fibres are highly ordered, thickened and settle out of solution. For the work presented here, we reasoned that replacing these few specific interactions with many more-general interactions would lead to networks of non-covalently cross-linked fibrils and, hence, physical hydrogels³, Fig. 1b.

The design rules for the hydrogelating SAF (hSAF) peptides initially followed those for the SAFs (ref. 8). That is, they were two-component systems based on the coiled-coil heptad sequence repeat, abcdefg. As the a, d, e and g positions are responsible for directing the dimer interface, Fig. 1, these were maintained from the original SAF design. Where the hSAFs differ from the original designs is at the b, c and f positions, which are exposed on the surfaces of the coiled-coil assemblies. For the hSAFs, these positions were made combinations of alanine and glutamine residues: alanine was chosen to promote weak hydrophobic interactions between fibrils, and glutamine for its propensity to hydrogen bond. Initially, three hSAF designs were investigated: variants hSAF_{AAA}, hSAF_{QQQ}

¹School of Chemistry, University of Bristol, Cantock's Close, Bristol, BS8 1TS, UK, ²Clinical Science at South Bristol, Level 7, Bristol Royal Infirmary, Bristol, BS2 8HW, UK, ³Unilever Corporate Research, Colworth Science Park, Sharnbrook, Bedford, MK44 1LQ, UK, ⁴Department of Physics, Cavendish Laboratory, J J Thomson Avenue, Cambridge, CB3 0HE, UK, ⁵Department of Chemistry and Biochemistry, School of Life Sciences, University of Sussex, Falmer, BN1 9QG, UK, ⁶Department of Biochemistry, University of Bristol, University Walk, Bristol, BS8 1TD, UK. *Present address: Department of Chemistry, University of Liverpool, Crown Street, Liverpool L69 7ZD, UK. †e-mail: d.n.woolfson@bristol.ac.uk; Michael.Butler@unilever.com.

Table 1 | hSAF amino-acid sequences.

Peptide name	Sequence
Heptad repeat	g abcdefg abcdefg abcdefg abcdef
hSAF _{AAA} p1	K IAALKAK IAALKAE IAALAEAE NAALEA
hSAF _{AAA} p2	K IAALKAK NAALKAE IAALAEAE IAALAE
hSAF _{QQQ} p1	K IQQLKQK IQQLKQE IQQLEQE NQQLEQ
hSAF _{QQQ} p2	K IQQLKQK NQQLKQE IQQLEQE IQQLEQ
hSAF _{AAQ} p1	K IAALKQK IAALKQE IAALQE NAALEQ
hSAF _{AAQ} p2	K IAALKQK NAALKQE IAALQE IAALQ
hSAF _{AAA-W} p1	K IAALKAK IAALKAE IAALWE NAALEA
hSAF _{AAA-W} p2	K IAALKAK NAALKAE IAALWE IAALAE

and hSAF_{AAQ}, Table 1, where subscripts denote amino acids at b, c and f, respectively. In hSAF_{AAQ}, which serves as a control, the pattern of alanine and glutamine residues was the same as for canonical positions in previous SAF designs.

Complementary hSAF peptides were mixed on ice, and either allowed to assemble at this temperature for 30 min, or removed after 5 min and incubated for 25 min at 20 °C. After these times, to test for gel formation, sample vials were inverted and incubated for a further 30 min without changing the temperature (see Supplementary Fig. S1). Through this simple test, hSAF_{AAA} and hSAF_{QQQ} both formed self-supporting gels. hSAF_{QQQ} formed a gel at low temperature, which melted on warming, whereas the hSAF_{AAA} formed a weak gel at low temperature that strengthened on warming. Moreover, this gel did not melt on heating up to 95 °C. The control, hSAF_{AAQ}, did not form gels.

To confirm and quantify the gel strengths, the storage (G') and loss (G'') moduli were recorded as a function of temperature using both microrheology (see Supplementary Fig. S2) and bulk oscillatory rheology, Fig. 2a. For both hSAF_{AAA} and hSAF_{QQQ}, G' was greater than G'' at low temperatures, confirming gel formation. However, whereas hSAF_{AAA} showed a slight increase in gel strength with temperature, hSAF_{QQQ} showed a transition to a liquid state between 16 and 19 °C, followed by a switch back to a gel state at higher temperatures.

The formation of fibrils within the hydrogels was confirmed by low-temperature field-emission scanning electron microscopy,

Fig. 2b–e. For both hSAF_{AAA} and hSAF_{QQQ}, the samples prepared on ice showed interconnected fibres with polydisperse widths, but without uninterrupted networks, Fig. 2b,c. Interestingly, on warming to room temperature, hSAF_{AAA} samples showed a homogeneous uninterrupted network of thinner fibres, Fig. 2e. The images for the control peptide, hSAF_{AAQ}, revealed no fibrous structures or networks, Fig. 2d, although unconnected fibres were visible by standard, negative-stain transmission electron microscopy of samples prepared at 20 °C (see Supplementary Fig. S3).

The peptide secondary structure and its packing in the fibril assemblies were probed by circular dichroism spectroscopy and X-ray fibre diffraction (XRD), respectively. Circular dichroism spectra recorded at 4 °C and 20 °C for both hSAF_{AAA} and hSAF_{QQQ} were characteristic of α -helical structure, Fig. 3a,c. That for the hSAF_{AAA} was the more intense and did not change on heating to 20 °C, whereas the spectrum for hSAF_{QQQ} lost intensity on heating and demonstrated distortion due to light scattering²⁰. These data are consistent with the gelation experiments described above.

XRD was carried out on hSAF_{AAA} at 20 °C and on hSAF_{QQQ} at 4 °C, Fig. 3b,d. In both cases, the diffraction patterns were similar to those presented for the other SAF systems¹⁹, although the unaligned fibres within the hSAF gels resulted in more-diffuse patterns with strong circular rings from water. hSAF_{AAA} and hSAF_{QQQ} gels both gave diffraction patterns with meridional reflections at 5.15 Å (M), corresponding to the 5.4 Å helical repeat of an α -helix supercoiled within a coiled coil.

The sharper meridional arc (M2) suggested some cross- β structure in the hSAF_{QQQ} sample²¹. We posit that this is probably due to the high glutamine content of this sequence, which favours amyloid-like assemblies in other systems^{22,23}. However, cross- β structure normally gives a stronger signal in XRD; thus, the comparatively weak reflection (E) in Fig. 3d, together with the predominantly α -helical circular dichroism spectrum, Fig. 3c, indicates only very small levels of β -structure in the hSAF_{QQQ} hydrogel.

Regarding the structural organization within the α -helical fibrils of the hSAF_{AAA} and low-temperature hSAF_{QQQ} gels, we have reported previously that for the standard, non-gelling SAFs the equatorial reflections (E) in the XRD, Fig. 3b,d, relate to the packing of the coiled coils on a hexagonal lattice¹⁹. Owing to overlap of some the reflections in the XRD data for the hSAF gels, however,

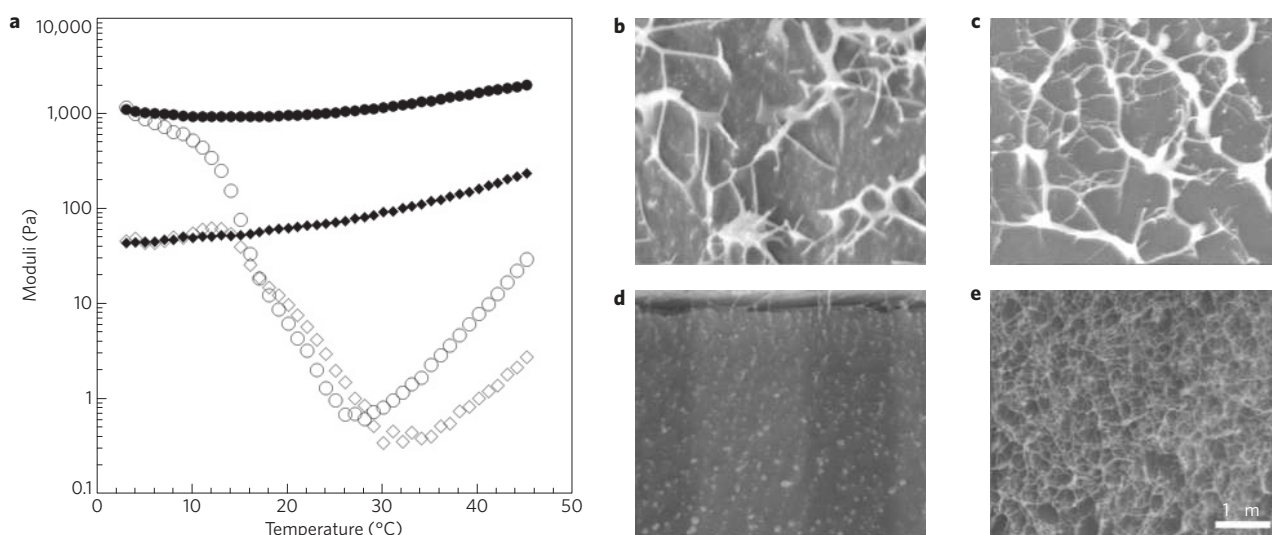


Figure 2 | Gel strength and network formation by the hSAFs. **a**, Gel strength gauged by non-destructive oscillatory rheology. G' , circles; G'' , diamonds; hSAF_{AAA}, filled symbols; hSAF_{QQQ}, open symbols. Measurements were made at a strain of 0.5%. **b–e**, Network formation as observed by cryogenic scanning electron microscopy for hSAF_{QQQ} (**b**), hSAF_{AAA} (**c**) and hSAF_{AAQ} (**d**), all assembled on ice for 15 min; and for hSAF_{AAA} assembled on ice for 3 min and then at room temperature for 12 min (**e**). All images are at the same magnification.

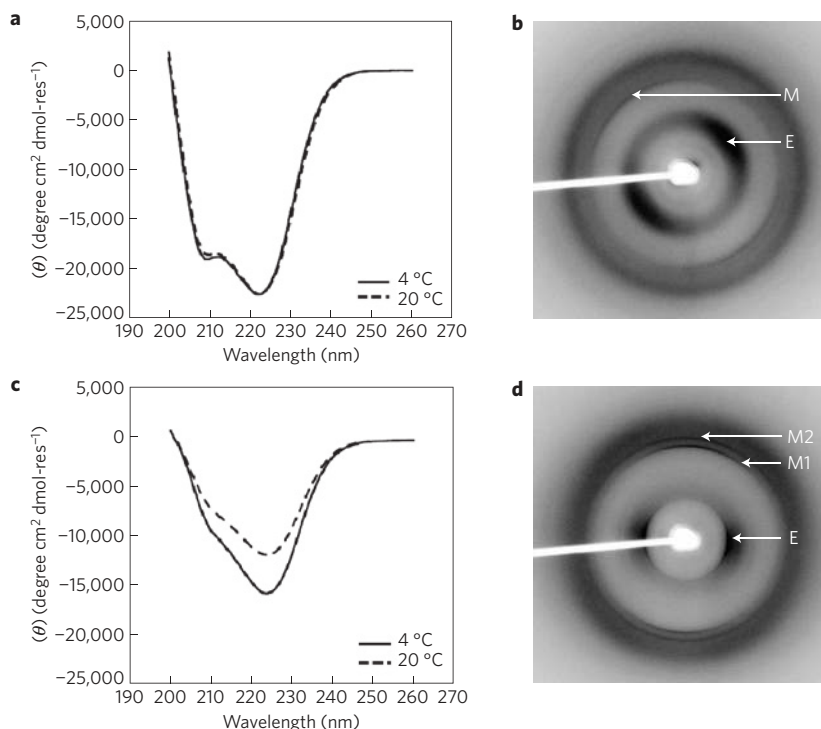


Figure 3 | α -helical secondary structure and packing within the fibrils and gels. **a–d**, Circular dichroism spectra (**a,c**) and X-ray fibre diffraction patterns (**b,d**) for hSAF_{AAA} (**a,b**) and hSAF_{QQQ} (**c,d**). In **b** and **d**, M and E refer to meridional and equatorial reflections, respectively.

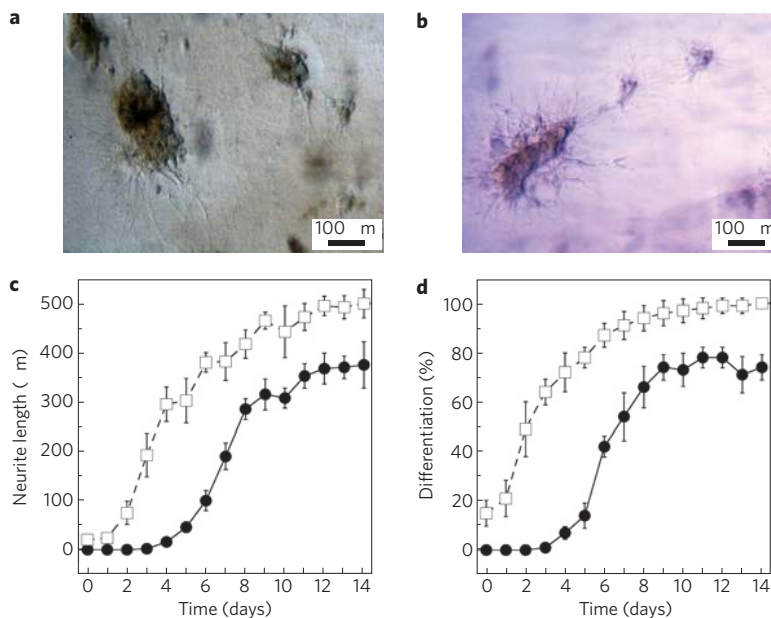


Figure 4 | Cell growth and differentiation on hSAF hydrogels. **a,b**, Phase-contrast microscopy of differentiating rat adrenal pheochromocytoma (PC12) cells in hSAF_{AAA-W} hydrogel (**a**) and Matrigel (**b**). These images were taken 10 days after adding nerve growth factor. Images from the full 14-day time course are given in the Supplementary Information. **c,d**, Cell differentiation as observed by neurite outgrowth was semi-quantified over time by the lengths of the processes (**c**) and the percentage of cells showing processes (**d**). Matrigel, open squares; hSAF gel, filled circles; the error bars show the standard error of the mean for measurements from at least 100 cells per cell cluster across 10 different fields of view in wells from three different plates.

it was not possible to index these arcs completely. Nonetheless, by comparison with our foregoing studies, it was possible to assess the packing distances between coiled coils in the gels. In the standard SAFs, coiled coils are 18.2 Å apart¹⁹. From the new data for hSAF_{AAA} and hSAF_{QQQ}, the corresponding separations were 17.3 Å and 21.5 Å, respectively. These spacings correlate with the changes to the sequences: for hSAF_{AAA}, closer packing is expected

because of the shorter alanine side chains, whereas in hSAF_{QQQ}, an increase might be expected because of (1) the replacement of predominantly alanine residues at b and c with the larger glutamine, and (2) the probable extra solvation of these hydrophilic residues. Circular dichroism spectra and XRD patterns, consistent with these assertions were obtained for the hSAF_{AAQ} control fibres (see Supplementary Fig. S4).

To probe the utility of the hSAF_{AAA} gels as a substrate for cell growth, we tested for peptide cytotoxicity and cell differentiation using rat adrenal pheochromocytoma (PC12) cells. First, however, we had to further stabilize the fibril–fibril interactions and the resulting gels. This was because, although hSAF_{AAA} gels could be washed and soaked in both phosphate-buffered saline and standard cell-culture media, they did not persist for sufficient time to allow sustained cell-culture experiments. To stabilize the gels, in each of the hSAF_{AAA} peptides we replaced one of the surface-exposed alanine residues at an f position with the more-hydrophobic tryptophan, Table 1. This also allowed easy quantification of peptide concentration. In all respects—spectroscopic, microscopic and gel formation—the hSAF_{AAA-W} combination behaved similarly to the parent peptides (see Supplementary Fig. S5). Moreover, the new peptides gelled at room temperature and the gels were stable in phosphate-buffered saline and cell-culture media at 37 °C for more than two weeks, which permitted cell-biology studies as follows.

In Alamar Blue cell-proliferation assays²⁴, PC12 cells were seeded on collagen and then treated with increasing concentrations (0.5–2.5 mM, equivalent to 1.5–7.5 mg ml⁻¹, total peptide) of hSAF_{AAA-W} peptides and gels proliferated, and were statistically no different to controls without peptide. This was in contrast to similarly prepared cells treated with staurosporine, a known inducer of apoptosis, which died (see Supplementary Fig. S6). Moreover, PC12 cells seeded on hSAF_{AAA-W} gels (without collagen) could be induced to differentiate into neural cells using nerve growth factor at 100 ng ml⁻¹ medium²⁵, as judged by the presence of neurite projections from the cell bodies, Fig. 4a. As shown by phase-contrast microscopy, Fig. 4a,b, the appearance of cells seeded on the hSAF_{AAA-W} gels was similar to those seeded on the widely used, but more-complex and *ex vivo* Matrigel²⁶ substrate. Despite also using Neuroscreen-1 cells, which are believed not to form aggregates, many of the induced cells ingressed the gels clustered in three dimensions, both with hSAFs and Matrigel, achieving three-dimensional cell cultures. Multiple images from the first 10 days of these comparative cell-culture experiments are given in Supplementary Fig. S7.

To compare cell differentiation within the hSAF and Matrigel substrates semi-quantitatively, we followed neurite extension with time, Fig. 4c, and gauged overall differentiation in each culture, Fig. 4d. A cell was defined to have differentiated if it had axodendritic processes longer than two cell body diameters in length, that is, processes longer than 20 µm (ref. 27). Although there was a lag in process growth and, consequently, cell differentiation in hSAF gels compared with Matrigel, on both counts the hSAF substrate performed at ~75% of Matrigel by 10 days. In making this comparison, it is important to bear in mind that hSAF is a well-defined *de novo* substrate without any of the natural structural proteins and associated cell-recognition motifs, or growth factors inherently present in Matrigel. Therefore, the performance of cells on hSAFs is particularly encouraging. In principle however, defined functionalities and extra factors could be engineered or added in known and controlled ways in future.

The hSAF peptides presented here gel at a peptide concentration of 1 mM (~3 mg ml⁻¹) in each peptide; that is, they have >99% water content. Moreover, as we have shown, changing the nature of the outer surfaces of the coiled coils—and, therefore, the inter-fibril interactions—enables temperature-responsive hydrogel properties to be engineered. This interesting and potentially useful behaviour warrants further comment. The hSAF_{QQQ} peptides, which have surface polar residues—that is, glutamine residues at the f positions of the coiled-coil repeat that have amide side chains and hydrogen-bonding potential—assemble to weak gels at low temperature and melt on warming. This is consistent with the breaking of weak hydrogen-bonded crosslinks between fibrils in a wet peptide gel. On the other hand, hSAF_{AAA} peptides—which

present only methyl side chains on their outer surfaces—form gels that become stronger on warming and are stable up to at least 95 °C. This is consistent with hydrophobic crosslinks between peptide fibrils. In contrast, the control peptides, hSAF_{AAQ}, in which the chemical uniformity of the outer surfaces is disrupted, do form fibres, but these do not form uninterrupted inter-fibril interactions and do not gel. Similar thermally responsive behaviour has been reported for an entirely different single-peptide hydrogelating system, namely, MAX3 and variants from the Schneider and Pochan team²⁸. In this case, the peptide is designed to form an antiparallel β -hairpin, which folds unimolecularly on heating and then assembles into amyloid-like fibrils that gel; the process reverses on cooling. Our observations of gelation by the hSAF system are fully consistent with our initial design principles for modifying the fibril surfaces, and further demonstrate that the rational design of increasingly complex biomaterial systems is possible through different routes.

Finally, our demonstration that hSAFs support cell growth and differentiation is encouraging for the application of these gels as straightforward, chemically defined and engineerable scaffolds for cell culture and tissue engineering. The hSAF systems also carry the distinct advantage that they have two peptide components, and, therefore, gel only on mixing. Thus, these new designs encompass unprecedented control, and represent an exciting addition to the available arsenal of biomaterials and gels.

Methods

Peptide synthesis. Peptides were synthesized on a CEM ‘Liberty’ peptide synthesizer using standard solid-phase 9-fluorenyl-methoxycarbonyl (Fmoc) chemistry. Amino acids were purchased from Novabiochem and other reagents from Rathburn Chemicals unless otherwise stated. Peptides were cleaved using 95% trifluoroacetic acid (Sigma), 2.5% triisopropylsilane (Sigma) and 2.5% 18.2 MΩ ultrapure water, purified by reverse-phase HPLC using acetonitrile (Fisher)–water gradients with 0.1% trifluoroacetic acid, and confirmed by matrix-assisted laser desorption/ionization–time of flight mass spectrometry. Pure peptides were freeze dried from acetic acid, weighed and dissolved in ultrapure water to give 3 mM (~9 mg ml⁻¹) stocks.

Circular dichroism spectroscopy. hSAF gels were prepared in 10 mM MOPS (Sigma) pH 7.0, at 1 mM (~3 mg ml⁻¹) of each peptide and incubated as described. All circular dichroism experiments were carried out in 0.01 cm quartz cells (Starna) using a Jasco J-810 circular dichroism spectrometer fitted with a Peltier temperature controller. Spectra were recorded between 190 and 260 nm with a 1 nm data pitch and bandwidth, 4 s response time, 50 nm min⁻¹ scanning speed and averaged over two accumulations. Baselines recorded using the same buffer, cell and parameters were subtracted from the data.

Electron microscopy. Low-temperature field-emission scanning electron microscopy was carried out using a JEOL 6301F microscope and Gatan Alto 2500 low-temperature equipment. Samples were mounted on brass rivets of 1 mm internal diameter. At set times, samples were frozen in nitrogen slush, and stored at –80 °C. These were mounted in a cooled holder (–196 °C), plunged into liquid nitrogen and transferred to the preparation chamber. These were then fractured using a cold scalpel tip and warmed to –90 °C for 30 s to remove a layer of ice. After re-cooling to –110 °C, samples were coated with 2 nm Pt/Pd and transferred to the microscope stage. For transmission electron microscopy experiments, 6 µl samples were placed on carbon-coated 400-mesh copper grids (Agar) on filter paper and dried, stained with 6 µl of filtered 1% uranyl acetate solution and examined in a Philips CM 100 microscope at 80 kV. Images were recorded using a Kodak Megaplug Camera 1.4i digital camera.

Rheology. Rheological measurements used an Anton Paar Physica RC 301 with an 8 mm parallel plate geometry, a Peltier plate and an environmental hood, with a 200 mm gap setting. G' and G'' were recorded using non-destructive oscillatory measurements at a strain of 0.5%, and over 3–45 °C. The measuring plate was surrounded by water to prevent drying of the sample. Samples were mixed *in situ* on the lower plate at 3 °C to total volumes of 300 µl, the geometry was lowered into position and samples incubated for 30 min.

XRD. Samples for X-ray fibre diffraction were prepared as previously described¹⁹. The hydrogels (10 µl) were suspended between two wax-filled capillaries, spaced ~1 mm apart and allowed to dry in air. The capillaries were gently separated and the fibre samples placed on a goniometer head. Diffraction data were collected using an R-Axis IV ++ detector and a Rigaku rotating anode with Cu K α radiation.

The specimen–detector distance was 160 mm, and the exposure time was 15 min. X-ray patterns were examined using Mosflm²⁹ and CLEARER³⁰.

Cell biology. Rat adrenal pheochromocytoma (PC12) cells and the subclone Neuroscreen-1 (ThermoFisher Scientific Celloomics) were used. Cells were maintained at 37 °C, 5% CO₂ in cell-culture medium comprising Dulbecco's Modified Eagle Media (DMEM, Invitrogen) supplemented with 10% (v/v) horse serum (Sigma), 5% (v/v) fetal bovine serum (Sigma), 1% (v/v) penicillin/streptomycin solution (Sigma) and 2 mM L-glutamine (Invitrogen). For the proliferation assays, cells were seeded at 1×10^4 cells cm⁻² in 96-well plates pre-coated with collagen solution (4 mg rat-tail type VII collagen (Sigma) dissolved in a filter-sterilized solution of 0.8 ml glacial acetic acid and 100 ml ultrapure H₂O, and activated before coating with 40 µl sterile 3.7% (w/v) NaCl per millilitre of collagen solution). After incubation for 24 h, the medium was replaced, and peptide (0.5, 1.0, 1.5, 2.0, 2.5 mM total) added. After 72 h, Alamar Blue dye (Serotec) was added (10% (v/v)) and incubated for 8 h. The fluorescence (excitation, 560 nm; emission, 590 nm) of 100 µl samples was measured. The ratio of the fluorescence intensities to that for a no-peptide control well was taken as a measure of cell proliferation. Another control used staurosporine (Sigma) to establish cell death. For the differentiation studies, ~ 1 cm² \times 2 mm hydrogel samples, which were 1 mM in each peptide, were prepared in phosphate-buffered saline (10 mM phosphate, 137 mM NaCl) and DMEM in 48-well dishes and left overnight. The gels were washed ($\times 6$) with cell-culture medium before seeding at 2×10^4 cells per well and leaving for 24 h. The medium was replaced and nerve growth factor (Sigma) added at 100 ng ml⁻¹ in DMEM. Matrigel (BD Biosciences) was prepared following the manufacturer's instructions, before washing and seeding similarly. Cells were followed for 2 weeks, with replacement of the medium and nerve growth factor every 3–4 days.

Received 15 December 2008; accepted 18 May 2009;
published online 22 June 2009

References

- Hirst, A. R., Escuder, B., Miravet, J. F. & Smith, D. K. High-tech applications of self-assembling supramolecular nanostructured gel-phase materials: From regenerative medicine to electronic devices. *Angew. Chem. Int. Ed.* **47**, 8002–8018 (2008).
- Woolfson, D. N. & Ryadnov, M. G. Peptide-based fibrous biomaterials: Some things old, new and borrowed. *Curr. Opin. Chem. Biol.* **10**, 559–567 (2006).
- Kopeček, J. & Yang, J. Y. Peptide-directed self-assembly of hydrogels. *Acta Biomater.* **5**, 805–816 (2009).
- Ulijn, R. V. & Smith, A. M. Designing peptide based nanomaterials. *Chem. Soc. Rev.* **37**, 664–675 (2008).
- Hirst, A. R. & Smith, D. K. Two-component gel-phase materials—highly tunable self-assembling systems. *Chem. Eur. J.* **11**, 5496–5508 (2005).
- Zhang, S. G., Holmes, T., Lockshin, C. & Rich, A. Spontaneous assembly of a self-complementary oligopeptide to form a stable macroscopic membrane. *Proc. Natl Acad. Sci. USA* **90**, 3334–3338 (1993).
- Aggeli, A. *et al.* Responsive gels formed by the spontaneous self-assembly of peptides into polymeric beta-sheet tapes. *Nature* **386**, 259–262 (1997).
- Pandya, M. J. *et al.* Sticky-end assembly of a designed peptide fiber provides insight into protein fibrillogenesis. *Biochemistry* **39**, 8728–8734 (2000).
- Hartgerink, J. D., Beniash, E. & Stupp, S. I. Self-assembly and mineralization of peptide-amphiphile nanofibers. *Science* **294**, 1684–1688 (2001).
- Schneider, J. P. *et al.* Responsive hydrogels from the intramolecular folding and self-assembly of a designed peptide. *J. Am. Chem. Soc.* **124**, 15030–15037 (2002).
- Paramonov, S., Gauba, V. & Hartgerink, J. Synthesis of collagen-like peptide polymers by native chemical ligation. *Macromolecules* **38**, 7555–7561 (2005).
- Petka, W. A., Harden, J. L., McGrath, K. P., Wirtz, D. & Tirrell, D. A. Reversible hydrogels from self-assembling artificial proteins. *Science* **281**, 389–392 (1998).
- Wang, C., Stewart, R. J. & Kopeček, J. Hybrid hydrogels assembled from synthetic polymers and coiled-coil protein domains. *Nature* **397**, 417–420 (1999).
- Potekhin, S. A. *et al.* De novo design of fibrils made of short alpha-helical coiled coil peptides. *Chem. Biol.* **8**, 1025–1032 (2001).
- Zimenkov, Y., Conticello, V. P., Guo, L. & Thiagarajan, P. Rational design of a nanoscale helical scaffold derived from self-assembly of a dimeric coiled coil motif. *Tetrahedron* **60**, 7237–7246 (2004).
- Dong, H., Paramonov, S. E. & Hartgerink, J. D. Self-assembly of alpha-helical coiled coil nanofibers. *J. Am. Chem. Soc.* **130**, 13691–13695 (2008).
- Gribbon, C. *et al.* MagicWand: A single, designed peptide that assembles to stable, ordered alpha-helical fibers. *Biochemistry* **47**, 10365–10371 (2008).
- Ryadnov, M. G. & Woolfson, D. N. Engineering the morphology of a self-assembling protein fibre. *Nature Mater.* **2**, 329–332 (2003).
- Papapostolou, D. *et al.* Engineering nanoscale order into a designed protein fiber. *Proc. Natl Acad. Sci. USA* **104**, 10853–10858 (2007).
- Papapostolou, D., Bromley, E. H., Bano, C. & Woolfson, D. N. Electrostatic control of thickness and stiffness in a designed protein fiber. *J. Am. Chem. Soc.* **130**, 5124–5130 (2008).
- Blake, C. & Serpell, L. Synchrotron X-ray studies suggest that the core of the transthyretin amyloid fibril is a continuous beta-sheet helix. *Structure* **4**, 989–998 (1996).
- Perutz, M. F., Johnson, T., Suzuki, M. & Finch, J. T. Glutamine repeats as polar zippers—their possible role in inherited neurodegenerative diseases. *Proc. Natl Acad. Sci. USA* **91**, 5355–5358 (1994).
- Sikorski, P. & Atkins, E. New model for crystalline polyglutamine assemblies and their connection with amyloid fibrils. *Biomacromolecules* **6**, 425–432 (2005).
- Hamid, R., Rotshteyn, Y., Rabadi, L., Parikh, R. & Bullock, P. Comparison of alamar blue and MTT assays for high through-put screening. *Toxicol. Vitro* **18**, 703–710 (2004).
- Drubin, D. G., Feinstein, S. C., Shooter, E. M. & Kirschner, M. W. Nerve growth-factor induced neurite outgrowth in PC12 cells involves the coordinate induction of microtubule assembly and assembly-promoting factors. *J. Cell Biol.* **101**, 1799–1807 (1985).
- Debnath, J., Muthuswamy, S. K. & Brugge, J. S. Morphogenesis and oncogenesis of MCF-10A mammary epithelial acini grown in three-dimensional basement membrane cultures. *Methods* **30**, 256–268 (2003).
- Todoroki, S., Morooka, H., Yamaguchi, M., Tsujita, T. & Sumikawa, K. Ropivacaine inhibits neurite outgrowth in PC-12 cells. *Anesth. Analg.* **99**, 828–832 (2004).
- Pochan, D. J. *et al.* Thermally reversible hydrogels via intramolecular folding and consequent self-assembly of a de novo designed peptide. *J. Am. Chem. Soc.* **125**, 11802–11803 (2003).
- Winn, M. D. An overview of the CCP4 project in protein crystallography: An example of a collaborative project. *J. Synchrotron Radiat.* **10**, 23–25 (2003).
- Makin, O. S., Sikorski, P. & Serpell, L. C. CLEARER: A new tool for the analysis of X-ray fibre diffraction patterns and diffraction simulation from atomic structural models. *J. Appl. Crystallogr.* **40**, 966–972 (2007).

Acknowledgements

We are grateful to the BBSRC (IIP0307/003), the Royal College of Surgeons of England (for a Shapurji H. Modi Memorial ENT Research Fellowship to support E.S.A.) and Unilever for financial support. We thank D. Dawbarn for the gift of the PC12 cells and S. Fuzeland and D. Atkins from Unilever for help with cryoEM.

Author contributions

E.F.B. and D.N.W. designed the peptides; E.F.B., E.S.A., D.J.A., M.F.B. and D.N.W. conceived and designed the experiments; E.F.B., E.S.A., A.C., M.K. and L.C.S. carried out the experiments; M.A.B. and A.M.D. co-supervised the cell biology and rheology, respectively; M.A.B. and M.F.B. co-supervised E.S.A. and E.F.B., respectively; D.N.W. coordinated, supervised and led the whole project; E.F.B. and D.N.W. wrote most of the paper.

Additional information

Supplementary information accompanies this paper on www.nature.com/naturematerials. Reprints and permissions information is available online at <http://npg.nature.com/reprintsandpermissions>. Correspondence and requests for materials should be addressed to M.F.B. or D.N.W.